JACS
JOURNAL OF THE AMERICAN CHEMICAL SOCIETY

Communication

pubs.acs.org/JACS

Observation of Superconductivity in Tetragonal FeS

Xiaofang Lai,[†] Hui Zhang,[‡] Yingqi Wang,[†] Xin Wang,[†] Xian Zhang,[†] Jianhua Lin,*[,†] and Fuqiang Huang*[,†,‡]

[†]Beijing National Laboratory for Molecular Sciences and State Key Laboratory of Rare Earth Materials Chemistry and Applications, College of Chemistry and Molecular Engineering, Peking University, Beijing 100871, China

[‡]CAS Key Laboratory of Materials for Energy Conversion and State Key Laboratory of High Performance Ceramics and Superfine Microstructure, Shanghai Institute of Ceramics, Chinese Academy of Sciences, Shanghai 200050, China

Supporting Information

ABSTRACT: The possibility of superconductivity in tetragonal FeS has attracted considerable interest because of its similarities to the FeSe superconductor. However, all efforts made to pursue superconductivity in tetragonal FeS have failed so far, and it remains controversial whether tetragonal FeS is metallic or semiconducting. Here we report the observation of superconductivity at 5 K in tetragonal FeS that is synthesized by the hydrothermal reaction of iron powder with sulfide solution. The obtained samples are highly crystalline and less air-sensitive, in contrast to those reported in the literature, which are meta-stable and air-sensitive. Magnetic and electrical properties measurements show that the samples behave as a paramagnetic metal in the normal state and exhibit superconductivity below 5 K. The high crystallinity and the stoichiometry of the samples play important roles in the observation of superconductivity. The present results demonstrate that tetragonal FeS is a promising new platform to realize high-temperature superconductors.

Layered iron chalcogenides have been of great interest due to their fascinating superconducting properties. For example, the superconducting transition temperature (T_c) of FeSe could be dramatically enhanced from 8 to 36.7 K under external pressure.[1] Moreover, T_c of the single-layer FeSe film on a $SrTiO_3$ substrate can reach as high as 65 K and greatly exceeds the bulk T_c of all known iron-based superconductors.[2] Another attractive aspect is that many high-T_c FeSe-derived superconductors could be realized by intercalating alkali metals, NH_3, organic solvent molecules, and even LiOH molecule into FeSe layers.[3] It is quite natural to search whether there exist other Se-free iron chalcogenides that exhibit superconductivity. Recently, the possibility of superconductivity in tetragonal FeS has attracted considerable attention because it is isostructural to the FeSe superconductor and shares many similarities with FeSe.[4] It is known that S substitution can enhance the superconducting transition temperature of FeSe and induce superconductivity in FeTe, which could be attributed to a modified local structure.[5] A remarkable feature in the FeAs-based superconductors is that T_c attains a maximum value when the $FeAs_4$ tetrahedra form a regular shape.[6] From that point of view, it is very likely tetragonal FeS becomes a superconductor with higher T_c than FeSe by virtue of its nearly regular FeS_4 tetrahedra.[7] Moreover, both Fe 3s core-level photoemission spectrum and density functional theory calculations indicate that there exist strong itinerant spin fluctuations in tetragonal FeS.[8] If spin fluctuations prove to be mediators of electron pairing,[9] tetragonal FeS could be a promising superconducting material.

However, all efforts made to pursue superconductivity in tetragonal FeS have failed so far, and it remains controversial whether tetragonal FeS is metallic or semiconducting. Density functional theory calculations suggest tetragonal FeS is a nonmagnetic metal, with electronic structure and Fermi surface similar to those of FeSe superconductor.[4,10] Experimentally, neutron diffraction and Mössbauer spectroscopy studies did not detect any magnetic ordering down to 4.2 K,[11] consistent with the magnetization measurements.[12] All electrical resistivity measurements revealed semiconducting rather than metallic properties for tetragonal FeS,[12b,c,13] while Denholme et al. observed a minimum in the temperature dependence of resistivity measured under high pressure and proposed that tetragonal FeS is intrinsically metallic, but due to a presence of weak localization, such metallic character is not exhibited below room temperature.[12c] To definitely define the physical properties of tetragonal FeS, single crystals are a necessity. Unlike FeSe and FeTe, synthesis of tetragonal FeS from elemental Fe and S has not been achieved.[14] Tetragonal FeS was usually prepared by iron corrosion in aqueous H_2S or coprecipitation of Fe^{2+} and S^{2-} at room temperature and ambient pressure.[12b,c,13,15] The samples thus obtained are very reactive toward oxygen and tend to transform into other iron sulfide phases that are more stable.[16] Therefore, it is desirable to find a more suitable synthetic route to high-quality tetragonal FeS.

Here, we report a new hydrothermal method to synthesize tetragonal FeS from iron powder and sulfide solution. X-ray diffraction, scanning electron microscopy, transmission electron microscopy, and X-ray photoelectron spectroscopy results reveal that the tetragonal FeS samples thus obtained are highly crystalline and less air-sensitive than those in the literature. Magnetic and electrical properties measurements show that tetragonal FeS has a paramagnetic and metallic normal state. For the first time, superconductivity was observed below 5 K, with superconducting volume fraction of 84% at 2 K. The upper critical magnetic field is estimated to be 0.4 T from the magneto-resistance measurements.

Received: June 28, 2015
Published: August 5, 2015

DOI: 10.1021/jacs.5b06687
J. Am. Chem. Soc. 2015, 137, 10148−10151

Single-phase samples of tetragonal FeS were prepared by the hydrothermal reaction of iron powder with sulfide solution. In a typical preparation run, 0.025 mol Fe powder and 0.025 mol $Na_2S{\cdot}9H_2O$ were placed in a 25 mL Teflon-lined autoclave. Deionized water was used to fill the autoclave to 60% of its capacity. The autoclave was then tightly closed and heated at 100−140 °C for 6 days. Following natural cooling to room temperature, the products were filtered, washed with deionized water, and dried at room temperature. All manipulations, except drying, which was conducted under vacuum, were performed in air. Powder X-ray diffraction (PXRD) data were collected on a Bruker D8 Focus X-ray diffractometer using Cu Kα radiation. Indexing and Rietveld refinement were performed using the DICVOL91[17] and FULLPROF[18] programs, respectively. Elemental analysis was carried out by inductively coupled plasma-atomic emission spectrometry (ICP-AES). Scanning electron microscopy (SEM) images were taken on a Hitachi S-4800 microscope. Transmission electron microscopy (TEM) images and selected area electron diffraction (SAED) patterns were obtained from a JEOL JEM-2100F microscope operating at 200 kV. X-ray photoelectron spectroscopy (XPS) measurements were performed on a Kratos Axis Ultra spectrometer using monochromatized Al Kα X-ray source. The magnetic susceptibility was measured with a magnetic field of 40 Oe, in both zero-field-cooling and field-cooling processes, and the electrical transport properties were measured through the standard four-wire method. These measurements were performed in a physical property measurement system (PPMS) of Quantum Design.

Chemical analysis for the tetragonal FeS sample by ICP-AES shows that the average atomic ratio is Fe/S = 1.03(2):1.0(1), and no other elements were detected. Figure 1 shows the PXRD

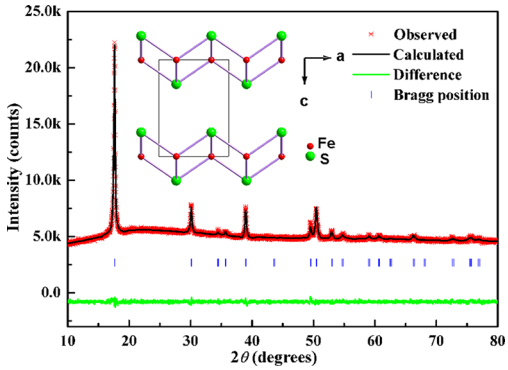

Figure 1. Rietveld refinement of the PXRD pattern of tetragonal FeS. Red small points represent the experimental values, black solid line is the calculated pattern, green solid line is the difference between the experimental and calculated values, and blue vertical bars are the Bragg positions. The inset shows the schematic crystal structure of tetragonal FeS (anti-PbO type).

pattern. No peaks due to impurities were observed. All the reflections can be well indexed based on a tetragonal cell with lattice parameters a = 3.6802(5) Å and c = 5.0307(7) Å, in good agreement with those reported in the literature.[12,13] Rietveld refinement using the reported tetragonal FeS model[14] gave satisfactory results. Shown in Figure 1 are the Rietveld refinement profiles, with agreement factors converged to R_p = 1.27%, R_{wp} = 1.62%, and χ^2 = 1.35. The refined structure parameters are summarized in Table 1. The inset of Figure 1 shows the schematic crystal structure of tetragonal FeS, which is composed of a stack of edge-sharing FeS_4 tetrahedra layer by

Table 1. Crystallographic Data of Tetragonal FeS[a]

atom	x	y	z	occupancy
Fe	0.75	0.25	0	1
S	0.25	0.25	0.2523(18)	1

[a]Space group $P4/nmm$, $a = b$ = 3.6802(5) Å, c = 5.0307(7) Å.

layer, without a spacer layer. The FeS_4 tetrahedron is nearly regular, with two S−Fe−S angles on the same side of ab plane being 110.8(2)°, which is just slightly larger than the ideal value (109.5°) for optimal superconductivity to occur in FeAs-based superconductors.[6]

The SEM image (Figure 2a) shows that the tetragonal FeS products form irregular thin microsheets with average edge

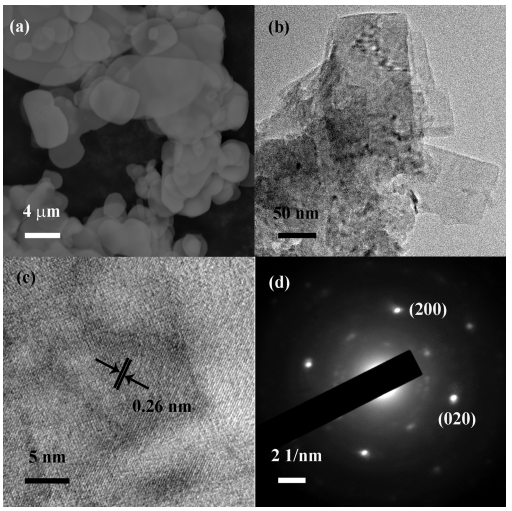

Figure 2. (a) SEM image, (b) TEM image, (c) high-resolution TEM image, and (d) SAED pattern along the [001] zone axis of tetragonal FeS.

length of several micrometers. However, the microsheets are not necessary single crystals, as significant aggregation often occurs in tetragonal FeS.[19] Smaller and thinner rectangular nanosheets can be obtained using ultrasonic cell grinder. Typical TEM image of such thinner nanosheets can be seen in Figure 2b. The size of the well-defined nanosheets is 50 nm or so. The high-resolution TEM image (Figure 2c) shows a set of high-resolution lattice planes with the interplanar distance of 0.26 nm, corresponding to the (110) plane of tetragonal FeS. The SAED spot pattern (Figure 2d) matches that predicted for the [001] direction of tetragonal FeS and can be indexed using $P4/nmm$ unit cell. These microscopy measurements confirm the formation of tetragonal FeS and indicate that the smaller and thinner FeS nanosheets shown in Figure 2b are single crystals.

Tetragonal FeS is usually reported to be amorphous or nanocrystalline and rather air-sensitive, as it is easy to be oxidized to Fe_3O_4 or decompose into other iron sulfide phases.[16,19] In comparison, our sample is highly crystalline and less air-sensitive. One possible reason is that the samples in previous studies are prepared either by precipitation of Fe^{2+} and S^{2-} at room temperature and ambient pressure[14] or by solvothermal[12a] or hydrothermal[16c] treatment of the FeS precursor, which is again obtained by precipitation; the nucleation is very fast. However, our sample is synthesized from iron powder and sulfide solution by the hydrothermal method; the nucleation is much slower, and this may be helpful to grow crystals with higher crystallinity and

DOI: 10.1021/jacs.5b06687
J. Am. Chem. Soc. 2015, 137, 10148−10151

fewer defects, which are more resistant to oxidation. XPS results (Figures S1−S3) reveal that our sample may be slightly oxidized on the surface. However, the PXRD pattern (Figure S4) of the sample exposed in air for over three months does not change much, which confirms that our sample oxidizes very slowly possibly due to smaller surface area, higher crystallinity, and fewer defects, and does not form any crystalline oxidized phases.

Figure 3 shows the temperature-dependent magnetic susceptibility measured under a magnetic field of 40 Oe. Unlike

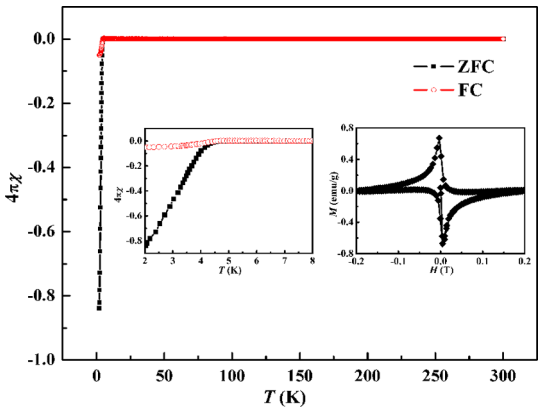

Figure 3. Temperature dependence of the direct-current magnetic susceptibility of tetragonal FeS measured under a magnetic field of 40 Oe, in both zero-field-cooling (ZFC) and field-cooling (FC) processes. The left inset shows the enlarged view of the temperature dependence of the magnetic susceptibility near the onset of superconducting transition. The right inset shows the magnetic hysteresis of the sample measured at 2 K.

the case in FeSe superconductor,[1a] no magnetic anomaly was observed around 105 K. In the high temperature range, the magnetic susceptibility is essentially flat and temperature independent, indicating that the sample is a Pauli paramagnet. Large diamagnetism due to superconductivity was observed below 4.5 K. The superconducting volume fraction estimated from the ZFC magnetic susceptibility at 2 K is 84%, confirming bulk superconductivity in the sample. Further confirmation of superconductivity is shown in the right inset of Figure 3, which displays the typical magnetic hysteresis curve for a type-II superconductor. As can be seen, both the lower and upper critical magnetic fields are very small in comparison with those of the other Fe-based superconductors.[1a,20]

Figure 4 shows the temperature-dependent electrical resistivity, measured on a cold-pressed pellet. In the high temperature range, the resistivity decreases linearly as temperature decreases, characteristic of metallic conductivity. This result supports the published first-principle calculations[4,10] but deviates from all the experimental electrical measurement results.[12b,c,13] One possible reason is that the samples reported in the literature are rather air-sensitive and the properties measured on them are flawed, while our sample is highly crystalline and less air-sensitive, and the properties measured on it are intrinsic. Apart from the metallic normal state, an abrupt decrease of resistivity was observed at 5 K, signaling the onset of superconductivity, and zero resistivity was reached at 4 K, consistent with the magnetization measurements. Superconducting transition temperature under a variety of magnetic fields was taken as the temperature where the resistivity drops to 50% of that at the onset (left inset of Figure 4). The right inset of Figure 4 shows the temperature dependence of the upper critical

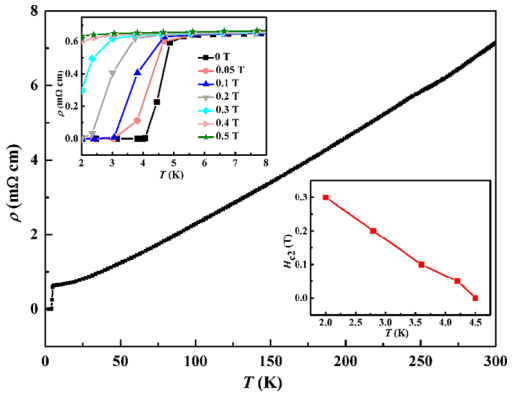

Figure 4. Temperature dependence of the electrical resistivity of tetragonal FeS. The left inset shows the electrical resistivity measured under magnetic fields of 0, 0.05, 0.1, 0.2, 0.3, 0.4, and 0.5 T below 8 K. The right inset displays the temperature dependence of the upper critical magnetic field.

magnetic field. According to the BCS theory, the upper critical magnetic field at $T = 0$ K can be determined by the Werthamer−Helfand−Hohenberg (WHH) formula $H_{c2}(0) = 0.693[-(dH_{c2}/dT)]_{Tc}T_c$.[21] Using $[-(dH_{c2}/dT)]_{Tc} = 0.12$ T K^{-1}, the estimated $H_{c2}(0)$ is 0.4 T, much smaller than that of FeSe superconductor (16.3 T).[1a]

Superconductivity can persist in the sample exposed in air for over three months, as shown in Figures S5 and S6. The high crystallinity and the stoichiometry of the sample may play important roles in the observation of superconductivity. On one hand, measurements on poorly crystalline samples can not reflect the intrinsic physical properties. On the other hand, similar to the case in FeSe and $Fe_yTe_{1-x}Se_x$, it has been suggested by first-principle calculations that excess iron incorporated in the structure of tetragonal FeS could disrupt any possible superconductive state.[22] This may be partly why superconductivity is observed in our sample, which is close to stoichiometric (indicated by ICP-AES result), rather than in the samples reported in the literature, which are usually metal-rich.[12,13] Meanwhile, the reduced excess iron in our sample also allows us to observe metallic normal state; otherwise excess iron would act as scattering points for conduction electrons and leads to localization effects as in the previous studies.[12c] The lower T_c of tetragonal FeS than FeSe is reasonable since besides the important factor-the regularity of FeX_4 (X = Se, S) tetrahedra, there are other factors that could affect T_c, such as the anion height, the strength of spin fluctuations, and the carrier density.[9c,23]

In conclusion, tetragonal FeS was successfully synthesized by the hydrothermal reaction of iron powder with sulfide solution. The obtained samples are highly crystalline and less air-sensitive, in contrast to those reported in the literature. SEM and TEM studies reveal that the samples are of microsheet morphology, which are aggregations of smaller well-defined single-crystal nanosheets. Based on the magnetic and electrical transport measurements, it is reasonable to conclude that tetragonal FeS behaves as a paramagnetic metal in the normal state. Bulk superconductivity at 5 K was discovered for the first time, with superconducting volume fraction of 84% at 2 K and the upper critical magnetic field $H_{c2}(0)$ of 0.4 T. The high crystallinity and the stoichiometry of the samples play important roles in the observation of superconductivity. Based on the high-quality tetragonal FeS, a series of FeS-derived superconductors with

DOI: 10.1021/jacs.5b06687
J. Am. Chem. Soc. 2015, 137, 10148−10151

higher T_c are expected by intercalating various spacer layers between FeS layers.

■ ASSOCIATED CONTENT

Supporting Information

The Supporting Information is available free of charge on the ACS Publications website at DOI: 10.1021/jacs.5b06687.

X-ray crystallographic data in CIF format for tetragonal FeS (CIF)

XPS spectra of tetragonal FeS (Figures S1–S3), PXRD pattern (Figure S4), and magnetization and electrical resistivity (Figures S5 and S6) of the sample exposed in air for over three months (PDF)

■ AUTHOR INFORMATION

Corresponding Authors

*huangfq@mail.sic.ac.cn

*jhlin@pku.edu.cn

Notes

The authors declare no competing financial interest.

■ ACKNOWLEDGMENTS

This work was financially supported by Innovation Program and "Strategic Priority Research Program (B)" of the Chinese Academy of Sciences (Grants KJCX2-EW-W11 and XDB04040200), National Natural Science Foundation of China (Grants 91122034, 51125006, 51202279, 61376056, and 21201012), and Science and Technology Commission of Shanghai (Grant 12XD1406800).

■ REFERENCES

(1) (a) Hsu, F. C.; Luo, J. Y.; Yeh, K. W.; Chen, T. K.; Huang, T. W.; Wu, P. M.; Lee, Y. C.; Huang, Y. L.; Chu, Y. Y.; Yan, D. C.; Wu, M. K. *Proc. Natl. Acad. Sci. U. S. A.* **2008**, *105*, 14262–14264. (b) Medvedev, S.; McQueen, T. M.; Troyan, I. A.; Palasyuk, T.; Eremets, M. I.; Cava, R. J.; Naghavi, S.; Casper, F.; Ksenofontov, V.; Wortmann, G.; Felser, C. *Nat. Mater.* **2009**, *8*, 630–633.

(2) (a) He, S. L.; He, J. F.; Zhang, W. H.; Zhao, L.; Liu, D. F.; Liu, X.; Mou, D. X.; Ou, Y. B.; Wang, Q. Y.; Li, Z.; Wang, L. L.; Peng, Y. Y.; Liu, Y.; Chen, C. Y.; Yu, L.; Liu, G. D.; Dong, X. L.; Zhang, J.; Chen, C. T.; Xu, Z. Y.; Chen, X.; Ma, X. C.; Xue, Q. K.; Zhou, X. J. *Nat. Mater.* **2013**, *12*, 605–610. (b) Tan, S. Y.; Zhang, Y.; Xia, M.; Ye, Z. R.; Chen, F.; Xie, X.; Peng, R.; Xu, D. F.; Fan, Q.; Xu, H. C.; Jiang, J.; Zhang, T.; Lai, X. C.; Xiang, T.; Hu, J. P.; Xie, B. P.; Feng, D. L. *Nat. Mater.* **2013**, *12*, 634–640.

(3) (a) Guo, J. G.; Jin, S. F.; Wang, G.; Wang, S. C.; Zhu, K. X.; Zhou, T. T.; He, M.; Chen, X. L. *Phys. Rev. B: Condens. Matter Mater. Phys.* **2010**, *82*, 180520. (b) Ying, T. P.; Chen, X. L.; Wang, G.; Jin, S. F.; Zhou, T. T.; Lai, X. F.; Zhang, H.; Wang, W. Y. *Sci. Rep.* **2012**, *2*, 426. (c) Ying, T. P.; Chen, X. L.; Wang, G.; Jin, S. F.; Lai, X. F.; Zhou, T. T.; Zhang, H.; Shen, S. J.; Wang, W. Y. *J. Am. Chem. Soc.* **2013**, *135*, 2951–2954. (d) Burrard-Lucas, M.; Free, D. G.; Sedlmaier, S. J.; Wright, J. D.; Cassidy, S. J.; Hara, Y.; Corkett, A. J.; Lancaster, T.; Baker, P. J.; Blundell, S. J.; Clarke, S. J. *Nat. Mater.* **2013**, *12*, 15–19. (e) Sedlmaier, S. J.; Cassidy, S. J.; Morris, R.; Drakopoulos, M.; Reinhard, C.; Moorhouse, S. J.; O'Hare, D.; Manuel, P.; Khalyavin, D.; Clarke, S. J. *J. Am. Chem. Soc.* **2014**, *136*, 630–633. (f) Guo, J. G.; Lei, H. C.; Hayashi, F.; Hosono, H. *Nat. Commun.* **2014**, *5*, 4756. (g) Biswas, P. K.; Krzton-Maziopa, A.; Khasanov, R.; Luetkens, H.; Pomjakushina, E.; Conder, K.; Amato, A. *Phys. Rev. Lett.* **2013**, *110*, 137003. (h) Lu, X. F.; Wang, N. Z.; Zhang, G. H.; Luo, X. G.; Ma, Z. M.; Lei, B.; Huang, F. Q.; Chen, X. H. *Phys. Rev. B: Condens. Matter Mater. Phys.* **2014**, *89*, 020507. (i) Pachmayr, U.; Nitsche, F.; Luetkens, H.; Kamusella, S.; Bruckner, F.; Sarkar, R.; Klauss, H.-H.; Johrendt, D. *Angew. Chem., Int. Ed.* **2015**, *54*, 293–297. (j) Lu, X. F.; Wang, N. Z.; Wu, H.; Wu, Y. P.; Zhao, D.; Zeng, X. Z.; Luo, X. G.; Wu, T.; Bao, W.; Zhang, G. H.; Huang, F. Q.; Huang, Q. Z.; Chen, X. H. *Nat. Mater.* **2014**, *14*, 325–329. (k) Sun, H.; Woodruff, D. N.; Cassidy, S. J; Allcroft, G. M.; Sedlmaier, S. J; Thompson, A. L.; Bingham, P. A.; Forderd Simon Cartenet, S. D.; Mary, N.; Ramos, S.; Foronda, F. R.; Williams, B. H.; Li, X.; Blundellf, S. J.; Clarke, S. J. *Inorg. Chem.* **2015**, *54*, 1958–1964. (l) Dong, X. L.; Zhou, H. X.; Yang, H. X.; Yuan, J.; Jin, K.; Zhou, F.; Yuan, D. N.; Wei, L. L.; Li, J. Q.; Wang, X. Q.; Zhang, G. M.; Zhao, Z. X. *J. Am. Chem. Soc.* **2015**, *137*, 66–69.

(4) Subedi, A.; Zhang, L. J.; Singh, D. J.; Du, M. H. *Phys. Rev. B: Condens. Matter Mater. Phys.* **2008**, *78*, 134514.

(5) (a) Mizuguchi, Y.; Tomioka, F.; Tsuda, S.; Yamaguchi, T.; Takano, Y. *J. Phys. Soc. Jpn.* **2009**, *78*, 074712. (b) Zajdel, P.; Hsieh, P.-Y.; Rodriguez, E. E.; Butch, N. P.; Magill, J. D.; Paglione, J.; Zavalij, P.; Suchomel, M. R.; Green, M. A. *J. Am. Chem. Soc.* **2010**, *132*, 13000–13007.

(6) Lee, C. H.; Kihoua, K.; Iyoa, A.; Kitoa, H.; Shirage, P. M.; Eisaki, H. *Solid State Commun.* **2012**, *152*, 644–648.

(7) Wilson, J. A. *J. Phys.: Condens. Matter* **2010**, *22*, 203201.

(8) Kwon, K. D.; Refson, K.; Bone, S.; Qiao, R.; Yang, W.-l.; Liu, Z.; Sposito, G. *Phys. Rev. B: Condens. Matter Mater. Phys.* **2011**, *83*, 064402.

(9) (a) Lumsden, M. D.; Christianson, A. D. *J. Phys.: Condens. Matter* **2010**, *22*, 203203. (b) Hanaguri, T.; Niitaka, S.; Kuroki, K.; Takagi, H. *Science* **2010**, *328*, 474. (c) Imai, T.; Ahilan, K.; Ning, F. L.; McQueen, T. M.; Cava, R. J. *Phys. Rev. Lett.* **2009**, *102*, 177005.

(10) Devey, A. J.; Grau-Crespo, R.; de Leeuw, N. H. *J. Phys. Chem. C* **2008**, *112*, 10960–10967.

(11) (a) Bertaut, E. F.; Burlet, P.; Chappert. *Solid State Commun.* **1965**, *3*, 335–338. (b) Vaughan, D. J.; Ridout, M. S. *J. Inorg. Nucl. Chem.* **1971**, *33*, 741–746.

(12) (a) Sines, I. T.; Vaughn, D. D., II; Misra, R.; Popczun, E. J.; Schaak, R. E. *J. Solid State Chem.* **2012**, *196*, 17–20. (b) Denholme, S. J.; Demura, S.; Okazaki, H.; Hara, H.; Deguchi, K.; Fujioka, M.; Ozaki, T.; Yamaguchi, T.; Takeya, H.; Takano, Y. *Mater. Chem. Phys.* **2014**, *147*, 50–56. (c) Denholme, S. J.; Okazaki, H.; Demura, S.; Deguchi, K.; Fujioka, M.; Yamaguchi, T.; Takeya, H.; ElMassalami, M.; Fujiwara, H.; Wakita, T.; Yokoya, T.; Takano, Y. *Sci. Technol. Adv. Mater.* **2014**, *15*, 055007.

(13) Zeng, S. L.; Wang, H. X.; Dong, C. *Chin. Phys. B* **2014**, *23*, 087203.

(14) Lennie, A. R.; Redfern, S. A. T.; Schofield, P. F.; Vaughan, D. J. *Mineral. Mag.* **1995**, *59*, 677–683.

(15) Berner, R. A. *Science* **1962**, *137*, 669.

(16) (a) Boursiquot, S.; Mullet, M.; Abdelmoula, M.; Génin, J.-M.; Ehrhardt, J.-J. *Phys. Chem. Miner.* **2001**, *28*, 600–611. (b) Lennie, A. R.; Redfern, S. A. T.; Champness, P. E.; Stoddart, C. P.; Schofield, P. F.; Vaughan, D. J. *Am. Mineral.* **1997**, *82*, 302–309. (c) Malasics, D. C.; Blanco, J. D. R.; Kis, V. K.; Rečnik, A.; Benning, L. G.; Pósfai, M. *Chem. Geol.* **2012**, *294–295*, 249–258.

(17) Boultif, A.; Louer, D. *J. Appl. Crystallogr.* **1991**, *24*, 987–993.

(18) Carvajal, J. R. *Physica B* **1993**, *192*, 55–69.

(19) (a) Jeong, H. Y.; Lee, J. H.; Hayes, K. F. *Geochim. Cosmochim. Acta* **2008**, *72*, 493–505. (b) Wolthers, M.; van der Gaast, S. J.; Rickard, D. *Am. Mineral.* **2003**, *88*, 2007–2015.

(20) (a) Tapp, J. H.; Tang, Z. J.; Lv, B.; Sasmal, K.; Lorenz, B.; Chu, P. C. W.; Guloy, A. M. *Phys. Rev. B: Condens. Matter Mater. Phys.* **2008**, *78*, 060505. (b) Zhu, X. Y.; Han, F.; Mu, G.; Cheng, P.; Shen, B.; Zeng, B.; Wen, H.-H. *Phys. Rev. B: Condens. Matter Mater. Phys.* **2009**, *79*, 220512.

(21) Werthamer, N. R.; Helfand, E.; Hohenberg, P. C. *Phys. Rev.* **1966**, *147*, 295.

(22) (a) McQueen, T. M.; Huang, Q.; Ksenofontov, V.; Felser, C.; Xu, Q.; Zandbergen, H.; Hor, Y. S.; Allred, J.; Williams, A. J.; Qu, D. *Phys. Rev. B: Condens. Matter Mater. Phys.* **2009**, *79*, 014522. (b) Bendele, M.; Babkevich, P.; Katrych, S.; Gvasaliya, S. N.; Pomjakushina, E.; Conder, K.; Roessli, B.; Boothroyd, A. T.; Khasanov, R.; Keller, H. *Phys. Rev. B: Condens. Matter Mater. Phys.* **2010**, *82*, 212504. (c) Brgoch, J.; Miller, G. J. *J. Phys. Chem. A* **2012**, *116*, 2234–2243.

(23) (a) Mizuguchi, Y.; Hara, Y.; Deguchi, K.; Tsuda, S.; Yamaguchi, T.; Takeda, K.; Kotegawa, H.; Tou, H.; Takano, Y. *Supercond. Sci. Technol.* **2010**, *23*, 054013. (b) Kamihara, Y.; Watanabe, T.; Hirano, M.; Hosono, H. *J. Am. Chem. Soc.* **2008**, *130*, 3296–3297.

DOI: 10.1021/jacs.5b06687
J. Am. Chem. Soc. 2015, 137, 10148–10151